Image Quality Improvement of Volume Hologram Printer with Digital Filter

（体積型ホログラムプリンタのディジタルフィルタによる画質改善に関する研究）

January, 2021

Computer Science Major

Graduate School of Science and Technology

Doctor Course

Nihon University

Hangbo Hua

(华 杭波)

Contents

1 Introduction **1**

1.1 Introduction 1

1.2 Relationship 2

1.3 Motivation 3

1.4 Overview of thesis 4

2 Background Knowledge **6**

2.1 Basic principles of optical holography 6

2.2 Wave-front record 6

2.3 Wave-front display 8

2.4 Computer-generated holography 8

2.5 Volume holography 9

2.6 Full-color volume hologram 9

2.7 Characteristic of holograms 10

2.8 Fringe printer 10

3 Volume hologram printer **12**

3.1 Introduction of volume hologram 12

3.2 Primary Plane Hologram 13

3.3 Calculation method 14

4 Volume hologram printer system **18**

4.1 Optical holographic printing system 18

4.2 Holographic wavefront printing system 19

4.3 Full-color volume hologram printer system 20

4.4 Volume hologram printer system 20

5 Improve quality of volume hologram **23**

5.1 Add digital filter to primary plane hologram 23

5.1.1 Image quality of printed volume hologram 23

5.1.2 Overlapping approach 24

5.1.3 Spatial digital filter 25

5.2 Partially overlapping to improve quality 27

6 Conclusion **32**

Bibliography **34**

Dedication **38**

Acknowledgments **39**

Publications **40**

List of Figures

2.1 calculation of hologram. 7
2.2 configuration of fringe printer. 11

3.1 Minimal system of the volume hologram printer [46]. Spatial filter is a combination of a microscope objective lens and a pinhole. . . 13
3.2 Model to create object data. 16
3.3 Schematic of the elemental hologram. 16
3.4 Configuration of computer-generated hologram (CGH) calculation and transfer. 17
3.5 Coordinates for virtual window in the final hologram plane. The reference point source for CGH is placed at the origin. 17

4.1 Distortion of the reconstructed image. 19
4.2 Schematic of full-color volume hologram printer system. 20
4.3 Modified 4f optics system between the PBS2 and the holographic plate. 21
4.4 Improved system of the volume hologram printer with $4f$ optics. . 22

5.1 (a) volume hologram in normal output (3D skull model). (b) Closeup of the middle part of the hologram as marked with rectangle in (a) 24
5.2 50 % overlapping approach in both horizontal and vertical directions. 25
5.3 Normal output with simply overlapping. 26
5.4 (a) Spatial filter to balance intensity on edges of the elemental volume hologram plane. (b) Closeup of the top right corner of the filter area as marked with rectangle in (a) 26
5.5 Comparisons of normal and filtered elemental hologram tiling. Horizontal axis represents x and vertical axis represents intensity of reconstructed image. Black lines show intensity of each elemental hologram and red lines show the total intensity. (**a**) Gap with normal edge; (**b**) Aligned with normal edge; (**c**) Overlap with normal edge; (**d**) Gap with filtered edge; (**e**) Aligned with filtered edge; (**f**) Overlap with filtered edge. 28
5.6 Partially overlapping approach 10% both in horizontal and vertical. 29
5.7 Reconstructed images from USAF-1951 resolution chart. 30
5.8 Reconstructed images from 3D skull holograms. 31

List of Tables

5.1 Simulation parameters based on the volume hologram printer . . . 27

Chapter 1

Introduction

1.1 Introduction

Holography [1] is to use the principle of interference and diffraction of light to superimpose coherent reference light waves on the object light waves to form interference patterns, and then record the interference patterns on the negative, develop the negative and use the original interference light to illuminate. Then the illumination light waves form the reproduction light waves similar to the original light waves after diffraction, thus displaying the 3D image containing all information of the object.

In 1948, Gabor [2, 3], a British Hungarian scientist, proposed the concept of holography based on the work of Bragg and Zernike in order to reduce the aberration of electron microscope and improve the resolution of image.（Holography was invented in 1948 by Hungarian physicist Dennis Gabor. The basic idea was that for perfect optical imaging, the total of all the information has to be used; not only the amplitude but also the phase.）Gabor envisions recording an exposure picture (i.e. hologram) of an electron wave diffracted by an object without passing through any lens, so that it can record all the information including the amplitude and phase of the object, and then use the reconstructed light wave to illuminate the hologram to obtain the enlarged object image. However, due to the limitation of experimental conditions at that time, we could only use mercury lamp to record in-line hologram, but the coherence of mercury lamp light source was poor, and the zero order, positive and negative first-order diffraction waves of coaxial hologram could not be separated. Therefore, from the proposal of holography to the end of 1950s, the research on holography had not made great progress. It was not until the emergence of laser in 1960 that Denisyuk [4], Leith and Upatnieks [5] used laser as coherent illumination source. Leith and others applied the theory of “side looking radar” in communication to optical holography and proposed off-axis holography. Holography entered a period of rapid development. They record the hologram by using off-axis reference light and object light interference, and irradiate the hologram with off-axis reconstruction light to obtain three space separated diffraction components [6, 7], so that the reconstructed original object image can be observed clearly. At the same time, they also used spatial filters in the optical system to eliminate stray light [8].

On this basis, scientists began to study the application of holography, including holographic display, holographic interferometry, holographic storage and holographic optical elements, and achieved a lot of resultsn [9–19]. In the late 1960s, Goodman et al. [20] proposed to use electronic technology and computer technology to realize the process of optical hologram recording and hologram reconstruction.

1.2 Relationship

Horman [21] first proposed the use of holography in interferometry. He described the use of a hologram element instead of the test section in the Mach Zehnder interferometer. Subsequently, Powell and Stetson [22, 23] proposed holographic interferometry for diffuse objects in the study of vibration analysis. The second exposure and real-time holographic interferometry were studied in several independent laboratories. Among them, Burch, Collier and Haine [24–26] have studied the deformation and displacement of diffuse scattering objects. Brooks and Heflenger [27] applied this method to the measurement of aerodynamics.

Holographic interferometry mainly includes static second exposure method, dynamic time average method and real-time method, holographic shearing interferometry, double reference light holographic interferometry and so on [28–39]. Among them, the second exposure method is to compare the initial object wave surface with the object light wave surface after the change of the object field. In the process of recording, a holographic plate is exposed twice. The hologram of the initial object light wave is recorded once, and the hologram of the changed object light wave is recorded once. The two holograms are recorded on the same dry plate. When irradiating with the original reference light wave, two object light wavefront can be reproduced. The two wavefront are coherent and the interference fringes between them can be observed. Through the distribution of interference fringes, we can know the change of wavefront. In the real-time method, the object is exposed once, and the holographic recording plate is accurately reset in the original photographic device after development, and the original interference light wave is used to irradiate. The reconstructed image will overlap on the original object. If the object has small displacement or deformation, interference fringes can be seen. Because the interference fringes appear regularly, it is called real-time holographic interferometry. In real-time holographic interferometry, it is very important to reset the holographic plate accurately, which brings some difficulties to the actual operation. For this reason, scientists have proposed to replace silver salt or gelatin dry plate with thermoplastic recording material, photorefractive crystal material and multiple quantum well recording material to improve recording conditions and achieve the purpose of rapid measurement.

Holographic interferometry has the following advantages [40]:

1. The amount of information recorded is large. Laser hologram has enough information capacity to record and reproduce some complex details with high fidelity. Therefore, holographic interferometry is not only suitable for measuring transparent objects, but also suitable for measuring three-dimensional diffuse reflection objects.

2. The amplitude is segmented in time. In general optical interferometry, the

beam from the same light source is divided into two coherent beams, that is to say, the beam is divided into two coherent beams, and the two coherent beams still exist at the same time in time. Holographic interferometry studies the interference of two spatially separated beams of coherent light. It uses the same spatial light to record the change information of an object at different times on the same holographic plate, and then the wavefront reconstructed at the same time interferes. The advantage of time division is that the coherent beam is generated by the same optical system, so the system error can be eliminated, the accuracy requirement of optical system for optical device can be reduced, and the installation and debugging of optical device are convenient.

3. Accuracy of records. Laser holographic interferometry is to compare the same object at different times by interferometry, so it can detect any small changes of the object in this period of time, and its accuracy can reach the order of magnitude of the light wavelength.

1.3 Motivation

In life, we can often see the application of holography technology. For example, in some credit cards and banknotes, there are ”Rainbow” holograms on polyester soft film produced by full-color hologram technology invented by Russian physicist Yuri danisuk in the 1960s. But these holograms are only used as a complex printing technology to achieve the purpose of anti-counterfeiting, their low sensitivity, color is not lifelike, far from the realm of the false. The researchers also tried to use dichromate glue as a photographic emulsion to make holographic recognition devices. Some fighters are equipped with such devices, which allow pilots to focus their attention on the enemy. Some precious cultural relics can be photographed with this technology. When displayed, the cultural relics can be reproduced in three dimensions for visitors to enjoy. The original objects are properly preserved to prevent theft. Large holograms can display cars, satellites and various three-dimensional advertisements, and pulse holography can be used to reappear portraits and wedding photos. A small hologram can be worn on the neck to form a beautiful decoration. It can reproduce people’s favorite animals, colorful flowers and butterflies. The rapid development of embossed rainbow hologram can not only become vivid cartoons, greeting cards, three-dimensional stamps, but also appear on trademarks, ID cards, bank credit cards and even banknotes as anti-counterfeiting marks. The three-dimensional hologram decorated in books, as well as the holographic rainbow shining on the gift packaging, make people realize the new leap of printing technology and packaging technology in the 21st century. Due to its three-dimensional sense of hierarchy, rainbow effect changing with the viewing angle, and the ever-changing anti-counterfeiting marks, as well as the close combination with other high-tech anti-counterfeiting means, the embossed holographic logo has pushed the anti-counterfeiting technology of the new century to a new brilliant peak.

In addition to optical holography, infrared, microwave and ultrasonic holography techniques have been developed, which are of great significance in military reconnaissance and surveillance. We know that the general radar can only detect the target's azimuth, distance, etc., while the hologram can give the three-dimensional image of the target, which is very important for the timely identification of aircraft, ships and so on. Therefore, people attach great importance to it. However, due to the rapid attenuation of visible light in the atmosphere or water, it can not even work in bad weather. In order to overcome this difficulty, infrared, microwave and ultrasonic holography techniques have been developed, that is, taking holograms with coherent infrared light, microwave and ultrasonic wave, and then reconstructing the object image with visible light. The principle of this holographic technology is the same as that of ordinary holography. The key of the technique is to find the medium of sensitive recording and the suitable reproducing method.

Holography has been extended from optical field to other fields. For example, microwave holography and acoustic holography have been greatly developed and successfully applied in industrial medical and other fields. The holography of seismic wave, electron wave and X-ray is also in-depth study. Holograms are widely used. For example, it is used to study shock wave of rocket flight and nondestructive test of honeycomb structure of aircraft wing. Now there are not only laser holography, but also white light holography, rainbow holography and panoramic rainbow holography, so that people can see all sides of the scene. Holographic three-dimensional display is developing towards holographic color stereoscopic TV and film. With the development of image processing technology, computer generated hologram (CGH) has been rapidly applied to various fields. Various of holograms has been printed, such as the computer-generated Fresnel hologram (CGFH), the computer-generated rainbow hologram (CGRH), the computer-generated cylindrical hologram (CGCH), the computer-generated disk hologram (CGDH), and the computer-generated alcove hologram (CGAH) [41].

1.4 Overview of thesis

The purpose of this paper is to use computer generated hologram (CGH) technology to print full-color volume holograms. Through the improvement of the software and hardware, the image quality of volume printing technology is improved. The following are the main contents of each chapter :

Chapter 1. Introduction

- A description of the history of volume hologram printer, related works and motivation

Chapter 2. Background Knowledge

- A description of the background of hologram. Introduction of principle and types of holograms.

Chapter 3. Volume hologram printer

- Sampling theory for the volume hologram. A description of steps about volume hologram printer.

Chapter 4. Volume hologram printer system

- Introduction of different kinds of hologram printer systems.

Chapter 5. Improve quality of volume hologram

- The method to improve the quality of out-put volume holograms. Add digital filter to the element hologram and partially overlapping.

Chapter 6. Conclusion

- Briefly summarizes the work and results done within this thesis, states areas in the system needing improvement, and discusses possible avenues of future research.

Chapter 2

Background Knowledge

With the development of computer technology and photoelectric imaging technology, computational holography and digital holography have gradually become the hotspots of holographic display research today, and the three-dimensional display and measurement technology based on wavefront reconstruction is gradually being used. Holographic optics is the foundation of all types of holographic technology. Optical holography uses optical interference to encode the wavefront into interference fringes, and then uses diffraction to reproduce the wavefront.

2.1 Basic principles of optical holography

Holography is a two-step lensless imaging method based on the principle of interference recording and diffraction reconstruction [42]. The wavefront of light from three-dimensional object is recorded on the photosensitive material. The hologram is illuminated according to the need to reproduce the wavefront of the previously recorded object light wave. It is a three-dimensional three-dimensional imaging technology.

2.2 Wave-front record

The first step of holography is to record all the amplitude and phase information of the object's light wave on the sensitive material. Since the photosensitive material is sensitive only to the intensity of light, coherent light is used to record the interference fringes generated by the mutual interference of object beam and reference beam with amplitude and phase information into a hologram in the form of intensity distribution, so the hologram is actually an interferogram.

Show in Figure 2.1, The object (O) is scattered by coherent light, and the scattered light carries all the information of the object. It is assumed that the coordinates of the object light wave and the reference light wave emitted by the coherent light source (R) arrive at the holographic plate H at x and y, respectively:

$$O(x,y) = O_o(x,y)\exp[i\phi_o(x,y)] \tag{2.1}$$

$$R(x,y) = R_r(x,y)\exp[i\phi_r(x,y)] \tag{2.2}$$

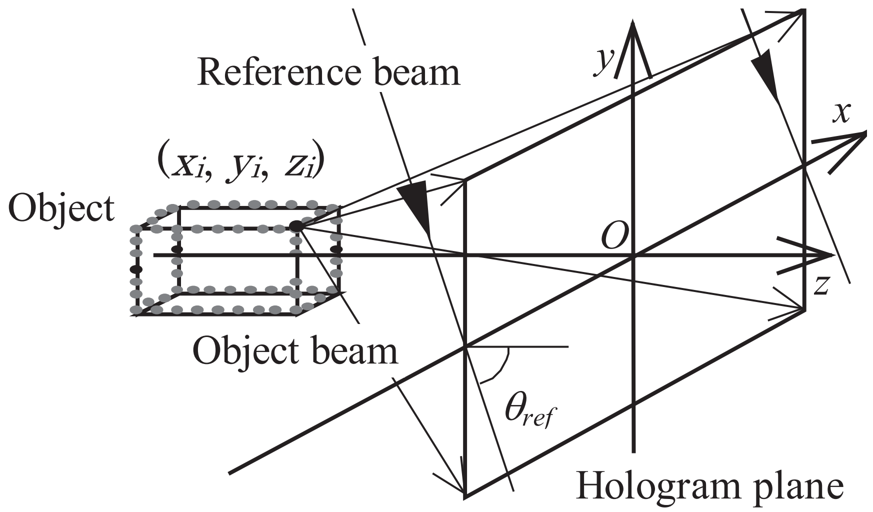

Figure 2.1: calculation of hologram.

where $O_o(x, y), R_r(x, y)$, $\phi_o(x, y)$ and $\phi_r(x, y)$ are the amplitude and phase distributions of the object wave and the reference wave on the H plane, respectively. Since the amplitude of light on the interference field is the coherent superposition of the two, the total light field on the H plane is :

$$U(x, y) = O(x, y) + R(x, y) \tag{2.3}$$

the intensity distribution after the interference is as follows :

$$\begin{aligned} I(X, Y) &= |O(X, Y) + R(X, Y)|^2 \\ &= |O|^2 + |R|^2 + 2\Re\{OR^*\} \\ &= |O|^2 + R_r^2 + 2O_oR_r \cos[\phi_r(x, y) - \phi_o(x, y)] \end{aligned} \tag{2.4}$$

In the above formula, the first term and the second term are the intensities of the reference light and the object light when they are separately on the plane h. their sum represents the average intensity of the interference fringes. The third term contains the amplitude and phase information of the object light wave and the reference light, which indicates that the intensity change of the interference fringes alternately is $2O_oR_r$. The phase is $\phi_r(x, y) - \phi_o(x, y)$. The amplitude information is obtained from the change of the visibility of interference fringes, and the phase information is obtained from the shape and spacing of interference fringes. Therefore, the interference fringes recorded on the hologram reflect all the information of the amplitude and phase of the object.

The transmission function t of hologram is proportional to the total light intensity, then the coefficient is assumed as a β :

$$\begin{aligned} t(x, y) &= \beta\,(|O|^2 + R_r^2 \\ &\quad +2O_oR_r \cos[\phi_r(x, y) - \phi_o(x, y)]) \end{aligned} \tag{2.5}$$

2.3 Wave-front display

The second step of holography is to display the object beam from hologram. The hologram can be regarded as a diffraction screen with a transmission coefficient of τ , which is equivalent to a composite grating, because this hologram records the distribution of object light field, which contains many gratings formed by coherent interference of plane wave and reference wave in different directions corresponding to different spatial frequency components. When a hologram is illuminated by a reference light, the reconstructed object beam waves are contained in the diffraction light field behind the hologram. After the amplitude distribution passing through the hologram plane H:

$$\begin{aligned} U_o(X, Y) &= R(x, y)t(x, y) \\ &= \beta\left(|O|^2 R + R_r^2 R + R^2 O^* + R_r^2 O\right) \end{aligned} \tag{2.6}$$

Where, the first and second term can be combined into one term, which retains the information of the reference wave beam. The third term and the original light wave only add a coefficient β to reproduce the object light wave, and the image formed is called the original image. The fourth term is the conjugate term, which not only conjugate with the object light wave, but also adds a phase factor. Therefore, this term becomes a distorted conjugate term and is a real image.

Each point on the hologram records all the information of the wave emitted by all points on the object, so each point can reproduce the whole image under the illumination of the reference light. The more points contribute to the reconstructed image, the higher the brightness of the image. The more points, the larger the illumination aperture, the higher the resolution of the image, and the wider the viewing angle of the three-dimensional image.

At the same time, the four items overlap each other on the hologram. Since light propagates independently, the four items overlapped on the hologram will propagate in three different directions. As long as the angle between these directions is large enough to be separated from the hologram, the images produced by these four items will not interfere with each other when observed in different directions.

2.4 Computer-generated holography

The hologram has three-dimensional (3D) information such as the binocular parallax, the convergence, and accommodation. Therefore, the reconstructed image of the hologram provides natural spatial effect. In particular, the viewer gets strong dimensional impression when the image is popping up from the hologram plane. Computer-generated holography (CGH) ,whose interference fringes are calculated on the computer, is a kind of technology which can form hologram by digital synthesis of object light wave. It does not need an actual object, as long as the mathematical information of the object light wave is input into the computer, the digital hologram is obtained after the computer coding, and then input into the spatial light modulator for direct display. CGH must first obtain the structure and texture data of the object. For the actual object, a digital three-dimensional scanner can be used for data collection. For non-existent objects, 3D software can be used to design the required three-dimensional objects and obtain three-dimensional data. In this paper, the data of three-dimensional objects are acquired by the existing 3D software, and the primary hologram is displayed through the spatial light modulator.

2.5 Volume holography

Due to the rapid development of computer technology, digital computer has been widely used in the field of optics. It can not only simulate the optical process, but also connect with the recording and display devices, and simulate most of the digital optical phenomena. At the same time, due to the emergence of fast Fourier transform (FFT) and other computing methods, the time required for calculation is greatly shortened, which provides the possibility for the application of computer technology in the field of holography, and promotes the development of hologram digitization technology. Since computer-generated hologram (CGH) is the calculated interference fringe pattern, which is made by the wave-front of a 3D object and the reference beam, and can faithfully reconstruct the recorded wave-front. However, the required pixel pitch almost as same as wavelength of visible light, the practical 3D display with the CGH printer could hardly be output. However, the common problem about those printers is those can only output a transmission hologram which is a plane interference fringe: although some of printers output the hologram which seems to be reflection type, it shows the transmission hologram on the character. The image which is reconstructed by the white light, will appears to be blurred. Because the transmission hologram is sensitive to the wavelength, as it has the wavelength selectivity. Then it is difficult to realize the full parallax and full color image. Therefore, for the full parallax and full color image reconstruction with the transmission hologram, the large-scale reconstruction system is necessary, which uses lights of primary color. As a method of the simple reconstruction, it is only necessary to use a volume reflection hologram. Since volume holograms have the wavelength selectivity, the full color image can be obtained with the white light illumination simply. The volume reflection hologram, however, needs an optical system to transfer a CGH.

2.6 Full-color volume hologram

The basic principle of color display is to decompose the image of a color object into three primary color images of red, green and blue and record them separately, and then superimpose the three primary color images through a certain method to achieve color display. Since color holography requires the superposition of three wavelengths of laser light to achieve display, there are also requirements on recording materials for recording holograms, and recording materials capable of simultaneously satisfying three colors of light are required.

2.7 Characteristic of holograms

Hologram is the result of the interference of scattered light and reference light which contains all information of the object, so the shape of interferogram is generally very complex. However, every point on the object can be regarded as the scattering center, radiating spherical or plane wavelet. Many of these wavelet superposition form a complex hologram. According to the recording and reconstruction of hologram, we can see that it has the following characteristics :

1. Holography can record and reproduce the amplitude and phase of the light wave of the object, so the stereoscopic image of the object can be obtained by holography

2. Holography is essentially an interference and diffraction phenomenon. The recording and reconstruction of hologram usually needs monochromatic light source, and the coherent length of monochromatic light should be greater than the optical path difference between object light wave and reference light wave, so as to ensure the interference between light wave scattered from different parts of the object and reference light wave

3. Any part of the hologram can reproduce the basic shape of the original object. The spherical wave scattered from any point of the object can reach each part of the holographic plate and interfere with the reference light to form a elementary hologram, that is, each point of the hologram records the scattered light from all the objects. So even if the hologram is damaged, it can reproduce the image of the object

2.8 Fringe printer

The zone plate technique proposed by Waters [43] synthesizes a computer generated hologram (CGH); a 3D image is represented by an aggregate of object points. Zone plates that generate the object points are summed to calculate a hologram distribution. This technique was inspired by the work of Rogers, who recognized that the Fresnel zone plate could be considered as a hologram [44]. With development of computer-generated hologram (CGH), fringe printer shown in Fig. 2.2 as the output device of the CGH, has developed to provide the 0.44 μm pitch and over 100 G-pixels holograms [45].

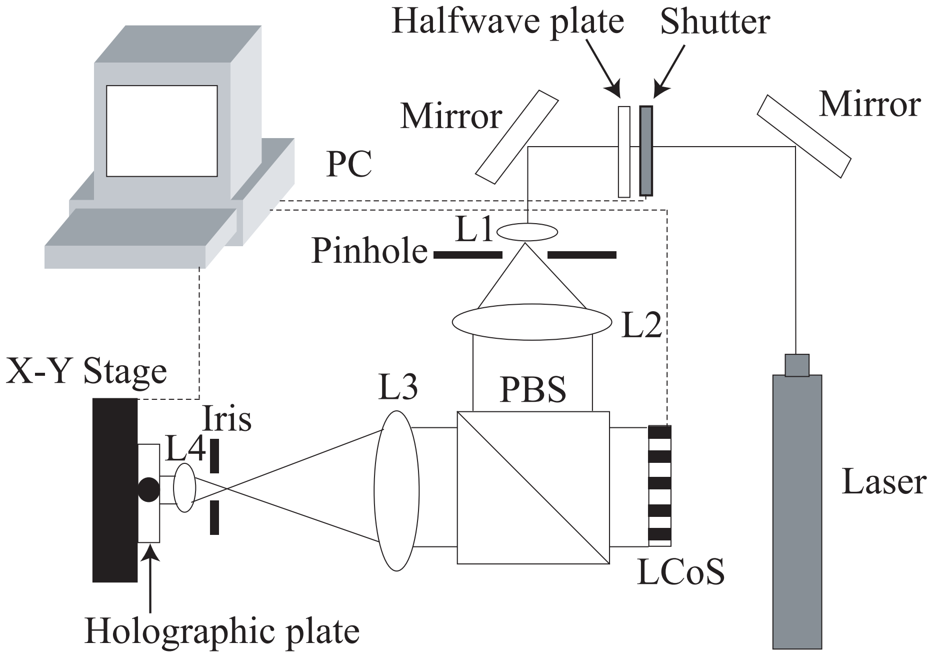

Figure 2.2: configuration of fringe printer.

Chapter 3

Volume hologram printer

Various kinds of hologram printers have been studied and holographic stereogram printers have been studied for many years and commercialized by several companies. The holographic stereograms are basically made from an array of 2D images, phase added stereograms include phase information to improve image quality and used to generate photo-realistic hologram. With developing of the computer-generated holograms (CGH) of 3D object, it becomes easier to calculate and print the plane transmission hologram. For CGH printing, an electron beam printer and a laser lithography provide quality printing. Since these equipment are high cost, some studies on low cost hologram printers have been proposed.

3.1 Introduction of volume hologram

Computer-generated hologram (CGH) is the calculated interference fringe pattern which is made by the wavefront of a 3D object and the reference beam, and can faithfully reconstruct the recorded wavefront. Since the required pixel pitch almost as same as wavelength of visible light, the practical 3D display with the CGH printer could hardly be output. Many researches have been conducted on the CGH printer, which has each feature, high resolution, high density, compact system, speedy print and so on. However, the common problem about those printers is those can only output a transmission hologram which is a plane interference fringe: although some of printers output the hologram which seems to be reflection type, it shows the transmission hologram on the character. The reconstructed image by the white light tends to get blurred and is difficult to realize the full parallax and full color image, since the transmission hologram does not have the wavelength selectivity. Therefore, for the full parallax and full color image reconstruction with the transmission hologram, the large-scale reconstruction system which uses lights of primary color is necessary. As a method of the simple reconstruction, it is only necessary to use a volume reflection hologram. Since volume holograms have the wavelength selectivity, the full color image can be obtained with the white light illumination simply. The volume reflection hologram, however, needs an optical system to transfer a CGH.

Although the plane transmission hologram is easy to print, it has a chromatic dispersion, which causes image blur with white light illumination. On the contrary, the volume reflection hologram has wavelength selectivity and causes no

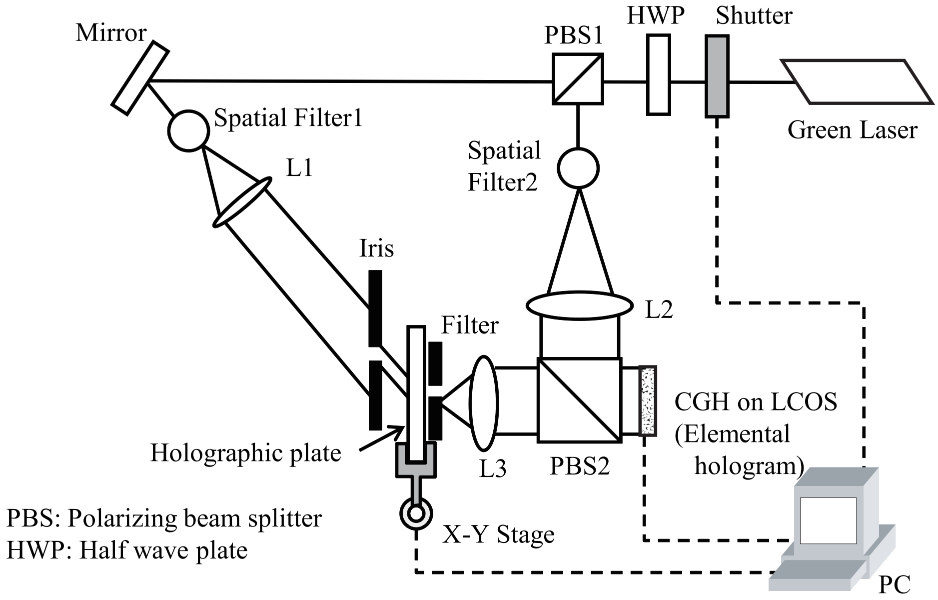

Figure 3.1: Minimal system of the volume hologram printer [46]. Spatial filter is a combination of a microscope objective lens and a pinhole.

chromatic dispersion and it's easy to show 3D images with white light illumination. Although the transmission hologram can be optically transferred to volume hologram manually, the automatic volume reflection hologram printer still have been studied. The main principle of volume hologram printer is a reconstructed image from the plane CGH is optically transferred to a photo-sensitive material as the volume reflection hologram. The volume hologram printer is also used to fabricate a holographic optical element for laser 3D display. Since the resolution of the spatial light modulator (SLM), which is used to display plane CGH, is usually megapixel order, the optically transferred volume hologram's size will be in mm order. Then, all of the mm order's transferred holograms are tiled to make a larger hologram. Since the volume hologram has 3D structure, it is not practical to calculate and print the volume hologram directly. Therefore, the plane hologram is calculated and its reconstructed image is transferred to volume hologram optically. Figure 3.1 shows a basic configuration of the volume hologram printer [46]. A part of the CGH is displayed on a Liquid Crystal on Silicon (LCOS) as the SLM. The reconstructed image from the CGH is transferred to a photo sensitive material with reference beam entering from the other side to make the volume reflection hologram as shown in Fig. 3.1. Since the transferred hologram is very small, many holograms are tiled to form a practical size hologram.The small transferred hologram is also called as an elemental hologram

3.2 Primary Plane Hologram

The reconstructed image from the CGH is recorded in a photo sensitive material (holographic plate) as the volume reflection hologram. This section describes calculation method of the primary plane hologram as CGH and digital filtering to record partially overlapped secondary volume hologram.

The object data represents a three-dimensional object, which is approximately a collection of self luminous points. The scheme consists of three-dimensional coordinates, amplitude and phase. Fig. 3.2 shows the model for creating object data. The observation point is located on the positive side of z axis. The three-dimensional object is located on the hologram plane, and the volume hologram is finally output. In addition, before computing the target data as the element hologram, the virtual window is used to segment the target data. As shown in the figure, the virtual window splits the hologram plane at equal intervals. In addition, an element hologram has an open virtual window. Only objects passing through the virtual window can be used to calculate the element hologram.

In other words, the element hologram records the object data segmented by the virtual window. In order to segment the target data in practical application, the recording area is added to the target point information one by one. The recording area is the area to be calculated for the target point on the element hologram. The figure 3.3 shows the model for calculating the recording area. If the light from the target point passes through both the open virtual window and the element hologram, the point is recorded on the element hologram. In order to calculate the recording area geometrically, we only consider the light passing through both ends of the open virtual window.

3.3 Calculation method

The primary plane hologram is calculated as the lensless Fourier hologram as show in Fig. 3.4.The volume hologram can be optically recorded from the CGH printed by the holographic fringe printer known as the optical transfer. The image reconstructed from the CGH is recorded in a photo sensitive material as the volume reflection hologram. Although the CGH can be recorded automatically, the optical transfer should be done manually. The basic idea of the volume hologram printer is replacing the printed CGH to the SLM. In this figure, it shows a model to calculate the elemental hologram as the lensless Fourier hologram. A reference point source is located under the open virtual window, and the object point source is used except for the dark zone. The elemental hologram is calculated by using the real part of the Fresnel hologram calculation as follows:

$$I(x,y) = \sum_{i=1}^{N} \frac{a_i}{r_i} \cos\{kr_i + \phi_R(x,y) + \phi_i\}, \tag{3.1}$$

where N is the number of the object points, a_i is the real-valued amplitude and ϕ_i is initial phase of the i-th object point. The wave number k is defined as $k = 2\pi/\lambda$, where λ is the free-space wavelength of the light. r_i is the distance between the i-th object point and the point $(x,\ y)$ on the elemental hologram, and ϕ_R is the phase distribution of the reference light. The intensity pattern of the light I is computed only in the record area of the object point. In addition, this calculation is necessary to satisfy the following equation:

$$2d(\sin\theta_{obj} - \sin\theta_{ref}) \leq \lambda, \tag{3.2}$$

where d is the pixel pitch of the elemental hologram, θ_{obj} is the angle of the object beam and θ_{ref} is the angle of the reference beam to the hologram. Among them, θ_{obj} and θ_{ref} are variable depending on the size of the virtual window. Therefore, the size of the virtual window is determined to satisfy Eq. (3.2).

In totally, the 3D object model is assumed as a collection of self-illuminated points. The sum of complex amplitudes from object points is interfered with the complex amplitude from the point reference source placed in the origin, or side of the object. Figure 3.5 shows a virtual window and a reference point source for CGH calculation. The virtual window has same size and position of the secondary volume hologram to avoid unnecessary calculation. The calculation is done only for light waves which pass the virtual window. The reconstructed image will appear at the same position of the original object when the CGH is illuminated with the conjugate wave of the reference wave. The conjugate image will also appear at the point symmetric position to the origin as shown in Figs. 3.5.

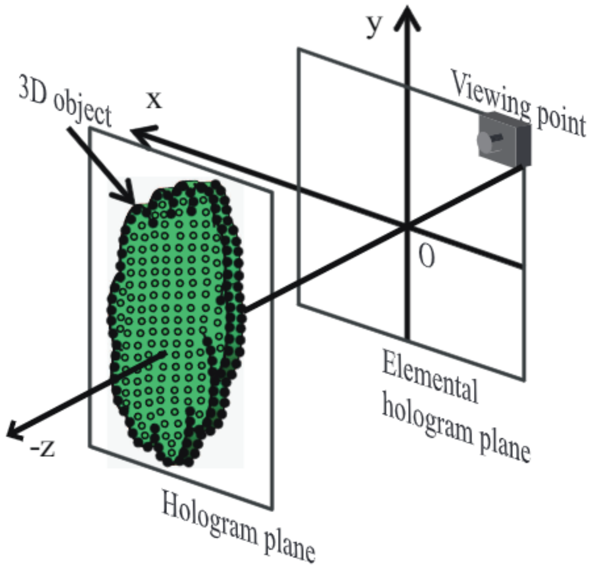

Figure 3.2: Model to create object data.

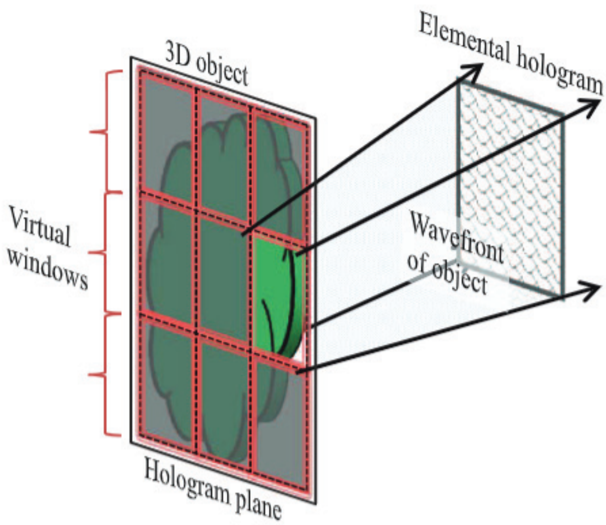

Figure 3.3: Schematic of the elemental hologram.

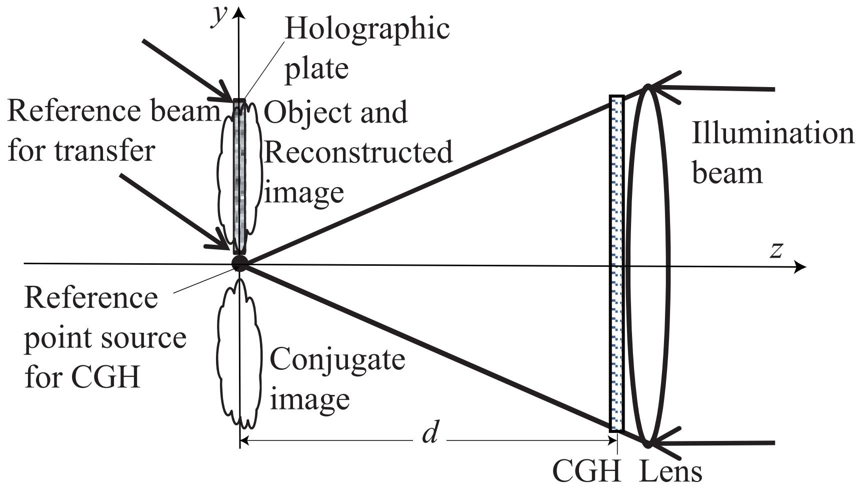

Figure 3.4: Configuration of computer-generated hologram (CGH) calculation and transfer.

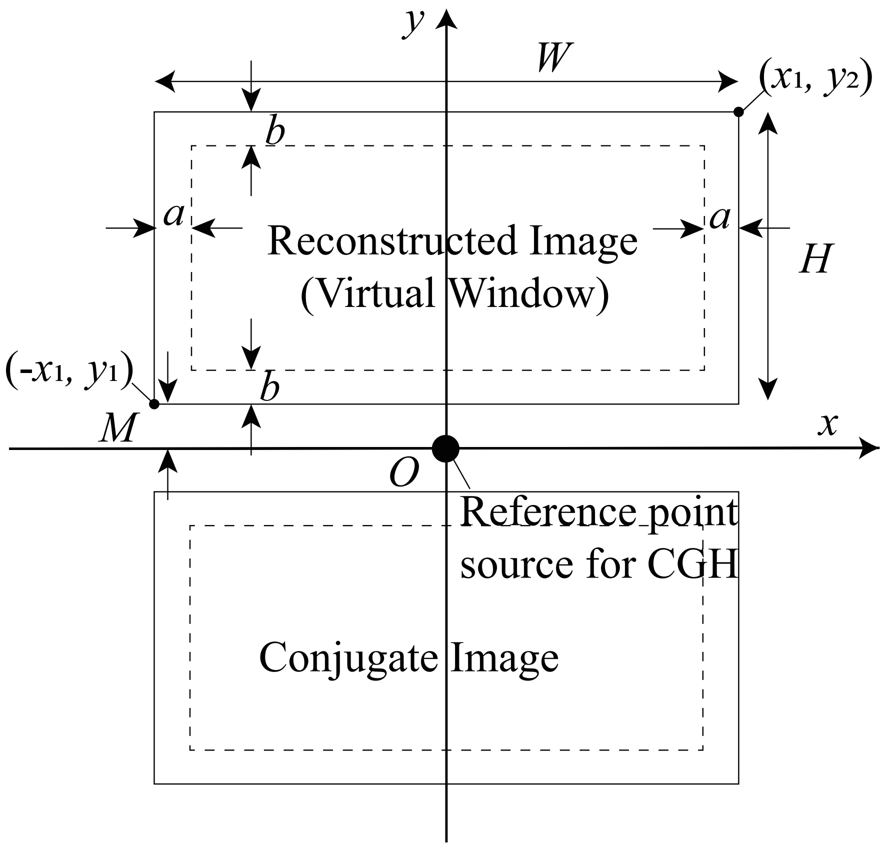

Figure 3.5: Coordinates for virtual window in the final hologram plane. The reference point source for CGH is placed at the origin.

Chapter 4

Volume hologram printer system

The field of static holographic three-dimensional display requirements is very wide, such as virtual display of precious cultural relics, static three-dimensional advertising, holographic three-dimensional topographic maps and holographic printing [47–52]. Due to the rapid development of computer technology and optoelectronic technology, the best solution for holographic display is to use computer and optoelectronic technology, combined with the characteristics of the hologram structure, to decompose the hologram into individual hologram units, and then use splicing technology Recorded on photosensitive material, this is the so-called hologram printing. Hologram printing technology has developed many technologies, and this article mainly introduces the full-color volume hologram printer.

4.1 Optical holographic printing system

The structure diagram of monochromatic source volume holographic printing system is shown in Fig. 3.1. After passing through the HWP, the light emitted by the laser is divided by the polarizing beam splitter PBS1. One way is the object light and the other is the reference light. After collimating and expanding, the reference beam passes through iris and reaches the holographic plate. After collimating and expanding, the object light is reflected by the polarizing beam splitter PBS2 and then vertically enters LCoS. Then the beam reaches the holographic plate through PBS2. Since the hologram is composed of multiple elemental holograms, the complete hologram can be printed by computer control platform X-Y.

The volume hologram is output when the reference beam from opposite side interferes with the reconstructed image of the elemental hologram on the LCoS. The important components of the minimal system are shown below: The L3, it's focal length is 50 mm and with a diameter of 45 mm, whose converging angle is proportionate to the viewing angel of output hologram; The filter can only passes the first order of the diffracted light from the LCoS; the LCoS's resolution is 1,920 by 1,080 pixels and it has 8 bits levels, which can displays the elemental hologram; the X-Y stage's resolution is 4 μm and it's moving area is 200 mm by 200 mm, which can translates the holographic plate; Shutter can control the exposure time. The behaviors of the volume hologram printer are, changing the displayed elemental hologram, switching the shutter to expose the hologram, translating the holographic plate and waiting the settling time to eliminate vibration settle. The personal computer is controlling a series of those behaviors. Thereby, the volume hologram can be output automatically.

In the minimal system, the reconstructed image of the elemental hologram has distortion due to the difference between the characteristic of the illumination beam and the calculation parameter of the reference beam. Figure **??** shows the appearance of reconstruction from the elemental hologram. If the Lens (L3) is located on the same position as the elemental hologram, the parallel illumination converges on the reference point and makes the object point reconstructed at its original position. However, the distance r between L3 and the elemental hologram actually is not able to be zero due to the thickness of the lens and PBS. Therefore, the reconstructed image is observed at the different position from the original position. The observed depth z' and the lateral magnification m are shown by the following equation:

$$z' = \frac{1}{\frac{1}{z} + \frac{r}{f^2}}, \tag{4.1}$$

$$m = \frac{z' + f}{z + f + \frac{rz}{f}}, \tag{4.2}$$

where z is the original depth of the object point. In other words, the more the reconstructed image has the depth and the more it becomes distorted. To cancel the distortion in the reconstruction, the 3D object should be pre-distorted by the basis of Eq. (4.1) and (4.2) before the calculation of the elemental hologram. In our experiment, $r = 100$ mm.

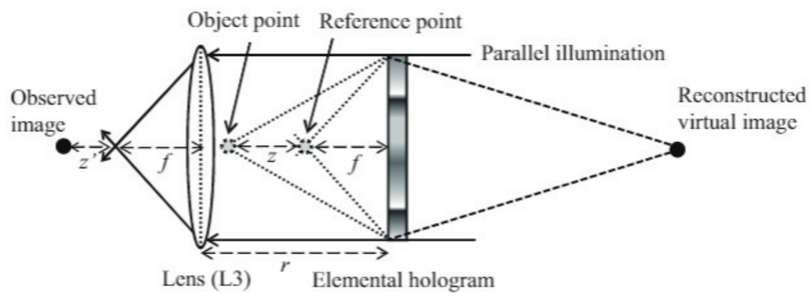

Figure 4.1: Distortion of the reconstructed image.

4.2 Holographic wavefront printing system

As we know, the reflection hologram can be reproduced under white light, and the holographic wavefront printing system can achieve this goal. The principle is

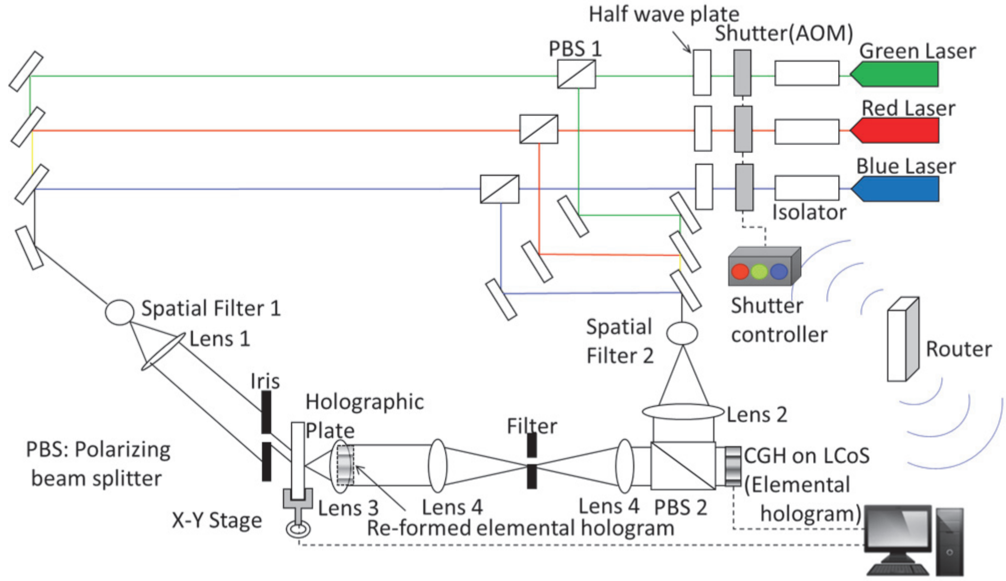

Figure 4.2: Schematic of full-color volume hologram printer system.

to load the computer hologram on the spatial light modulator LCoS (as the SLM), diffract the image after laser illumination, and then pass the band-pass filter to get the wavefront of the image. Then take this wavefront as the object light. Through interfering the reference light with it, we can get the reflection hologram and record it. The figure below shows the light path structure diagram. It can be seen that the holographic wavefront printer inputs the elemental holograms into Liquid Crystal on Silicon (LCoS), and the lenses L1 and L2 form a 4F system, which reduces the image displayed on the LCoS onto the recording plane. Among them, there is a spatial spectrum plane in the 4f system, and a band-pass filter is placed on this plane to pass only the spectrum of the reproduced image. In this way, the light distribution on the recording plane is no longer elemental holograms, but object light waves. At the same time, the reference light is introduced behind the recording material to interfere with the object light wave, and the reflection hologram can be recorded. Its biggest advantage is that it can achieve white light reproduction.

4.3 Full-color volume hologram printer system

Full-color volume hologram has been introduced by another research group [53], it is synthesized by three monochromatic light sources, so the system needs to split and combine the red, green and blue lasers at the same time. Figure 4.2 shows our proposed system.

4.4 Volume hologram printer system

The volume hologram can be optically recorded from the CGH printed by the holographic fringe printer as shown in Fig. 3.4, known as the optical transfer. The

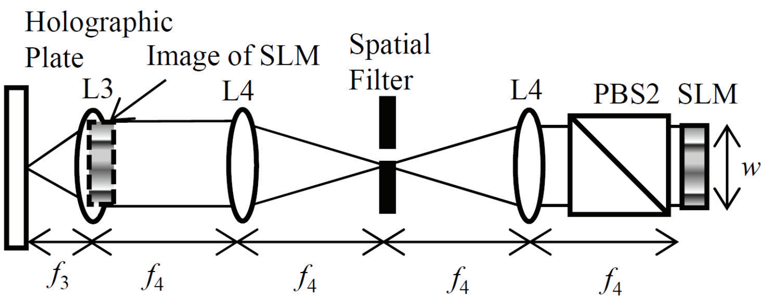

Figure 4.3: Modified 4f optics system between the PBS2 and the holographic plate.

image reconstructed from the CGH is recorded in a photo sensitive material as the volume reflection hologram. Although the CGH can be recorded automatically, the optical transfer should be done manually. The basic idea of the volume hologram printer is replacing the printed CGH to the SLM. A part of the CGH is displayed on the LCoS as the SLM and the reconstructed image from the LCoS is transferred to the unexposed holographic plate. The CGH is calculated as the lensless Fourier hologram. The calculation method is same as the Fresnel hologram with a point reference light located beside of the 3D object. Although an amplitude modulation type LCoS can be used for the SLM, a phase-only LCoS is also used to provide a complex amplitude modulation. Similar to the holographic fringe printer, the single transferred hologram is as small as square millimeters. Therefore, the X-Y stage translates the plate and printing numbers of the elemental transferred hologram to make the reasonable size volume hologram. The same control system designed for the holographic fringe printer can be used for the volume hologram printer.

In the minimal system, The focal length f_3 of the lens L3 in Fig. 3.1 is the key of the optical system. The maximum size of the elemental transferred hologram takes the same value of $\delta_{\max}$ in Fig. 3.4. Therefore, the longer f_3 provides the larger elemental transferred hologram and it makes printing rate higher. On the other hand, the f_3 also determine the viewing angle Θ, where the reconstructed image can be observed, written as,

$$\Theta = 2\tan^{-1}\frac{w}{2f_3}, \tag{4.3}$$

where w is the size of the SLM. The larger f_3 reduces the viewing angle, compromising with the elemental transferred hologram size. As shown in Fig. 3.4, the lens L3 should be placed close to the CGH to avoid distortion in the reconstructed image. However, it is difficult for the printer configuration shown in Fig. 3.1 because the PBS2 is inserted between the SLM and the lens L3. Therefore, it is better to insert the $4f$ optical system to relay the image of the SLM onto the L3 as illustrated in Fig. 4.3.

The improved volume hologram printing system is shown in Fig.4.4. These two L4s' focal length is 100 mm and diameter is 40 mm. The rest are same with Fig. 3.1.

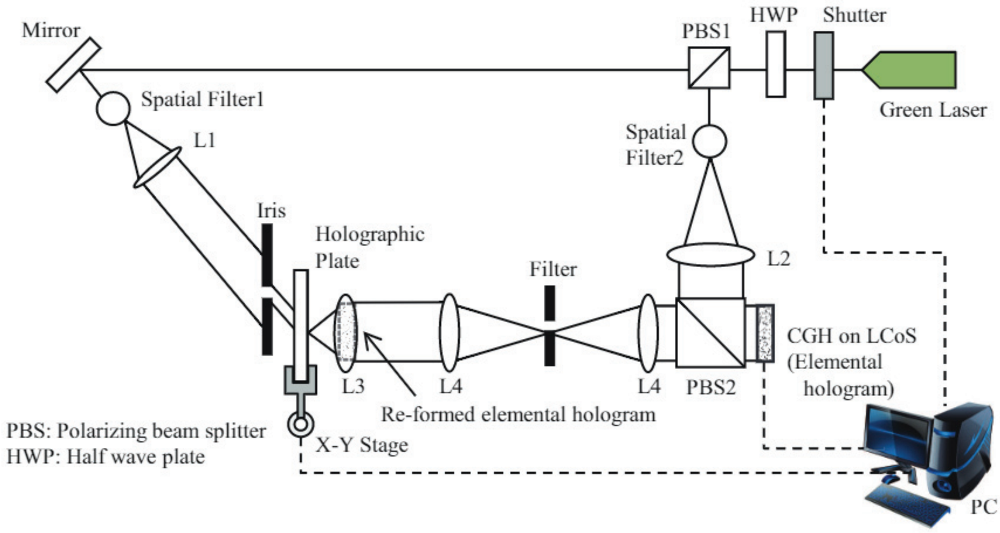

Figure 4.4: Improved system of the volume hologram printer with $4f$ optics.

Chapter 5

Improve quality of volume hologram

The volume hologram printer is useful for 3D display, because it is selective to the wavelength and be able to reconstruct with the natural illumination. But the final volume hologram consists of tiled small holograms and the tiling manner often causes spilt lines which will have impact on image quality. In order to improve this influence, this chapter introduces digital filter and Partially overlapping in detail.

5.1 Add digital filter to primary plane hologram

According to the previous description, in the volume hologram printing process, the SLM is replaced by the primary hologram produced by CGH transmission. When printing a complete hologram, due to the resolution of the optical system and other reasons, it is necessary to divide the hologram into several elemental holograms in the process of calculating point data.

5.1.1 Image quality of printed volume hologram

Since the resolution of the spatial light modulator (SLM) , which is used to display plane CGH, is usually megapixel order, the optically transferred volume hologram's size will also be in mm order. Then, all of the mm order's transferred holograms are tiled to make a larger hologram. This tiling manner is recorded by using X-Y motorized stage. In the improved optical system, a computer is used to control the X-Y motorized stage. In the computer control panel, we can adjust the exposure time when printing, the printing order of elemental hologram, etc. However, when moving the X-Y motorized stage, it will cause phase discontinuity and image degradation in reconstruction by diffraction effect at each elemental hologram.

Using this volume hologram printer, a 3D model of skull is printed shown in Fig.5.1. In general, the hologram can be printed completed. This volume hologram consists of tiled small holograms and the tiling manner often causes spilt lines shown in Fig.(b), which will reduce the quality.

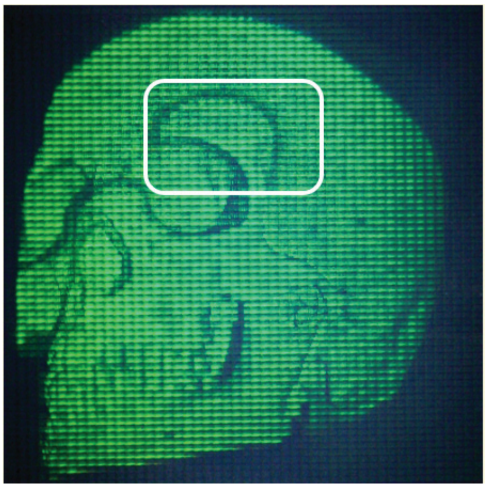

(a)

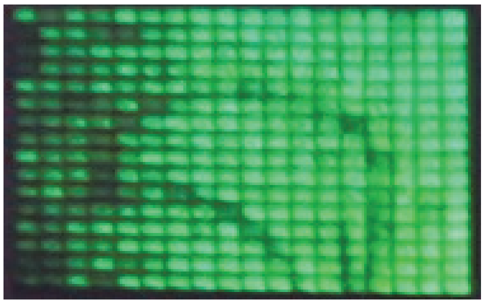

(b)

Figure 5.1: (a) volume hologram in normal output (3D skull model). (b) Closeup of the middle part of the hologram as marked with rectangle in (a) .

5.1.2 Overlapping approach

Within a elemental hologram region, the wavefront reproduced by CGH can be recorded. However, the dividing process of the entire hologram causes the phase discontinuity at the split lines of each elemental hologram, due to a lack of positioning accuracy of X-Y motorized stage and also the time incoherence recording of them. Because of this phase discontinuity, the reconstructed image will be degraded by undesired diffraction effect. However since previous works of wavefront printer do not optimize the cell size, the reconstructed images were degraded by obtrusive split line due to visible cell size caused by too large cell size for human eyesight, or by diffraction effect due to discontinuity of phase distribution caused by too small cell size. For this case, the overlapping recording approach of sub-holograms is proposed to achieve both conditions: enough smallness of apparent cell size to make cells invisible and enough largeness of recording cell size to suppress diffraction effect by keeping the phase continuity of reconstructed wavefront [55]. Fully overlapping approach is proposed and the overlap ratio is 50 % in both horizontal and vertical directions in that approach [55].

Fig.5.2 shows the concept of proposed approach. It is assumed that the entire hologram data is divided into M × N of sub-hologram data considering an overlapping mentioned. The first exposure of sub-hologram cell (0, 0) is executed on the hologram, recording film with the cell size of S_H. In the region of one exposure, since the recorded wavefront of object light is reproduced from a single SLM, continuity of phase distribution in this region is ensured. Next exposure position of sub-hologram cell (1, 0) is shifted by D_S from sub-hologram cell (0, 0) to X-axis. After recording M times of sub-holograms to X-axis with same shift value D_S, the exposure position of sub-hologram cell (0, 1) is shifted D_S to Yaxis. Then M times of exposure of second line are executed. A repetition of N lines of exposures in the same manner as the first line, the entire hologram can be recorded on the hologram recording film. In the overlapping approach, the phase continuity of wavefront is ensured within the cell size S_H, and the appearance

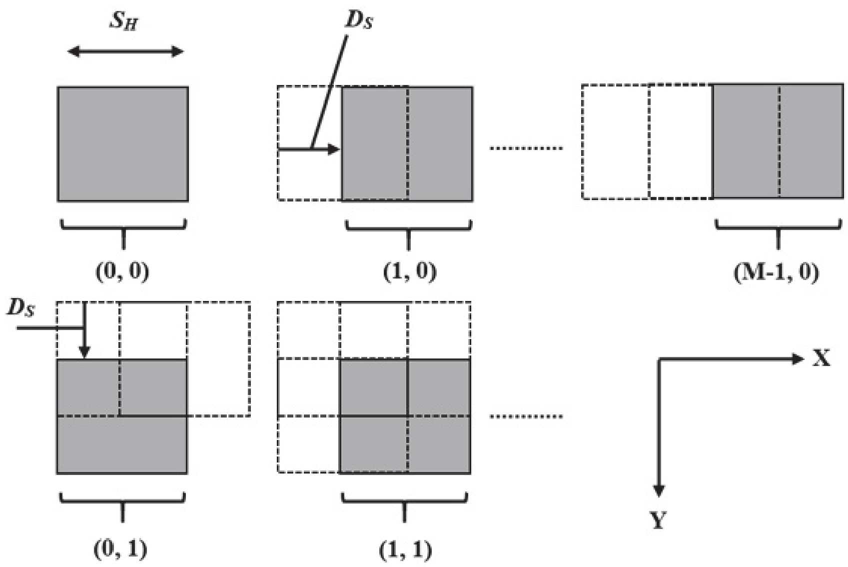

Figure 5.2: 50 % overlapping approach in both horizontal and vertical directions.

cell size becomes at D_S. Therefore, both parameters can be set independently, and to optimize D_S smaller than S_H, it is possible to keep both conditions.

5.1.3 Spatial digital filter

If the mm order's transferred holograms are simply overlapped partially, there will have strong intensity non-uniformity (higher intensity in the overlapped parts than the non-overlapped parts) that causes the split lines and reduces the quality. Fig.5.3 shows the normal output which is simply overlapped. The split lines between elemental holograms are obviously. To improve this case, the intensity non-uniformity of the overlapped part should be counterbalanced to make it continues. The reconstructed image, which is the result of the first hologram calculated as lensless Fourier hologram, should reduce image intensity near its edges. In consideration of this, a digital filter is applied to the overlapping area to control image intensity.

For a uniform intensity, the first hologram, which has been Fourier transformed, is multiplied with a spatial digital filter as shown in Fig. 5.4(a), then inverse Fourier transformed to obtain filtered or intensity controlled hologram.

The amplitude distribution of the filter is defined as:

$$f(x, y) = f_x(x) f_y(y). \tag{5.1}$$

Square of $f_x(x)$ and square of $f_y(y)$ are table shape function and written as:

$$f_x(x) = \begin{cases} 0 & (x < -x_1) \\ \sqrt{(x_1 + x)/a} & (-x_1 \leq x < -x_1 + a) \\ 1 & (-x_1 + a \leq x < x_1 - a) \\ \sqrt{(x_1 - x)/a} & (x_1 - a \leq x < x_1) \\ 0 & (x_1 \leq x) \end{cases} \tag{5.2}$$

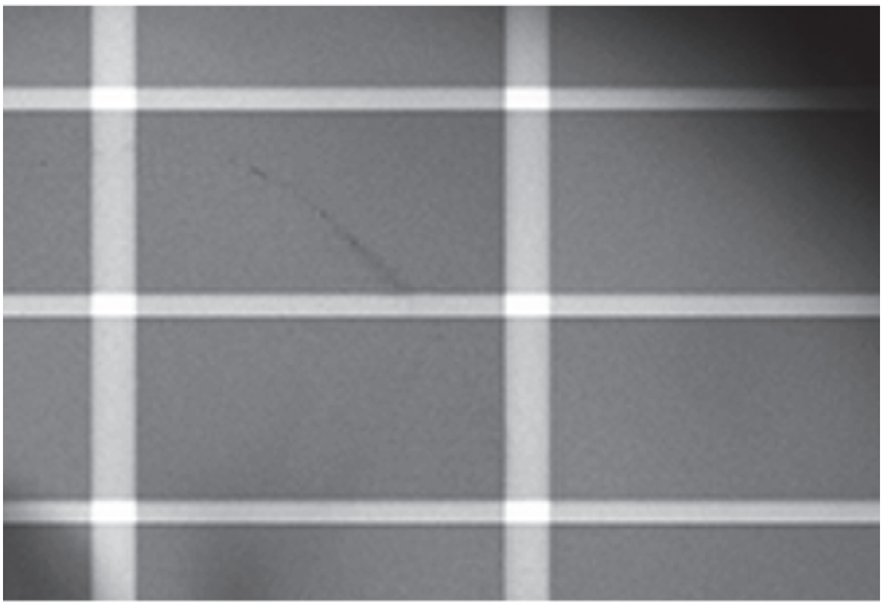

Figure 5.3: Normal output with simply overlapping.

(a) (b)

Figure 5.4: (a) Spatial filter to balance intensity on edges of the elemental volume hologram plane. (b) Closeup of the top right corner of the filter area as marked with rectangle in (a) .

where a is an overlapping width, and $-x_1$ and x_1 are left and right coordinates of the reconstructed image plane shown in Figure 3.5. The horizontal overlap ratio is defined as a/W.

$$f_y(y) = \begin{cases} f_y(|y|) & (0 \leq y) \\ 0 & (0 < y < y_1) \\ \sqrt{(y - y_1)/b} & (y_1 \leq y \leq y_1 + b) \\ 1 & (y_1 + b < y < y_2 - b) \\ \sqrt{(y_2 - x)/b} & (y_2 - b \leq y \leq y_2) \\ 0 & (y > y_2) \end{cases} \tag{5.3}$$

where b is an overlapping height, and y_1 and y_2 are bottom and top coordinates of the reconstructed image plane shown in Fig. 3.5. The vertical overlap ratio is defined as b/H. Figure 5.4(a) is a sample of digital spatial filter image in intensity ($\propto f^2(x, y)$) whose resolution is same as the first hologram (4,096 × 2160 pixel). Overlapping ratios defined below are 10 % in horizontal and 10 % in vertical.

The white and gray parts are the window of reconstructed image plane. Black part is outside of the window with a value of zero. The middle White part is non-overlapped with a value of one. The gray part around the its edge is overlapped part with a value changes gradually from one to zero. Figure 5.4(b) shows the closeup of the top right filter area as marked with rectangle in Figure 5.4(a).

Based on Figure 5.4 and Eq. (5.2), two different types of hologram tiling are shown in Fig. 5.5. Fig. 5.5(a), (b) and (c) are normal edge in three kind joints and Fig. 5.5(d), (e) and (f) are filtered ones. Though in normal ones, well joint with edge as shown in Fig. 5.5(b) can solve the intensity problem and have good results in simulation, the quality of printed hologram also has problems in calculation of points data. The filtered ones, which is used to improve the quality, show three kind results in gap, aligned and overlapped. Fig. 5.5(d) and (f) are insufficient overlap and excessive overlap. Similar with normal edge, the insufficient and excessive ones will cause the intensity distribution uneven. Lower intensity with black gaps between elemental hologram and higher intensity with overlaps. Comparison of these cases, Fig. 5.5(e) is well aligned with filtered edge. Filtered hologram can solve the problem of image intensity caused by miss alignment and reduce the influence of calculation problem.

5.2 Partially overlapping to improve quality

Nevertheless, when using 50 % overlapping approach (in both horizontal and vertical directions), the printing speed is reduced one quarter as normal. As the printing speed is slower, it will takes too much time to print a large hologram. To improve image quality with little loss in printing speed, partially overlapping approach was proposed. Figure 5.6 shows the partially overlapping approach proposed here(10% both in horizontal and vertical). The principle is similar with 50% overlapping approach.

Numerical simulations are performed with parameters listed in Table 5.1, based on the volume hologram printer in the author's lab.

Figure 5.7 shows numerical reconstruction simulations of 2D model (USAF-1951 resolution chart) from normal, overlapped holograms without filter and with filter. In these results, the spatial digital filter is applied to each elemental hologram and the intensity near edges is balanced. Although the simulation has been done with perfect alignment of elemental holograms, visible dark gaps between

Table 5.1: Simulation parameters based on the volume hologram printer

Item	Value
Laser wavelength	532 nm
CGH (LCOS) pixels	4,096 × 2,160
CGH (LCOS) pixel pitch	4.0 μm
Distance d between CGH and virtual window (Focal length of L3)	40 mm
Virtual window width W	4.0 mm
Virtual window height H	2.0 mm
Offset of virtual window M	0.2 mm

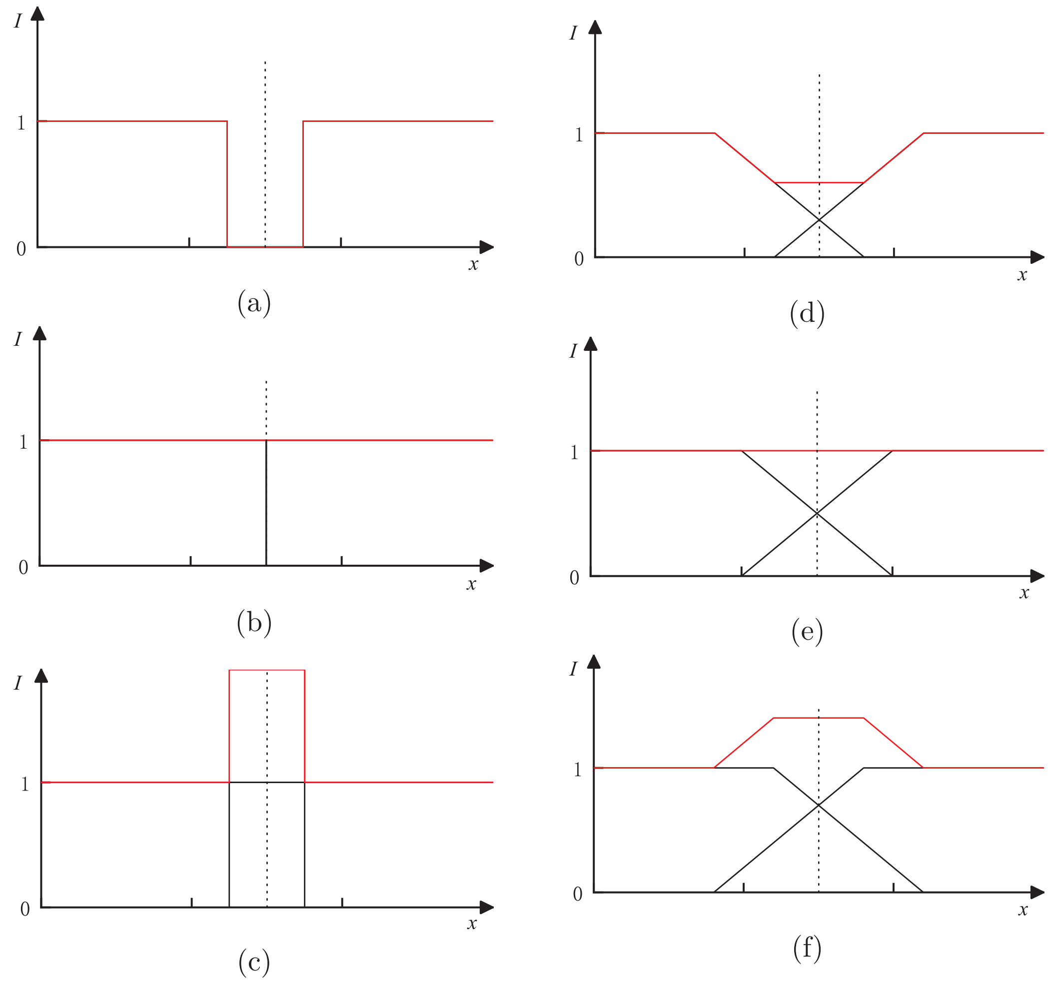

Figure 5.5: Comparisons of normal and filtered elemental hologram tiling. Horizontal axis represents x and vertical axis represents intensity of reconstructed image. Black lines show intensity of each elemental hologram and red lines show the total intensity. (**a**) Gap with normal edge; (**b**) Aligned with normal edge; (**c**) Overlap with normal edge; (**d**) Gap with filtered edge; (**e**) Aligned with filtered edge; (**f**) Overlap with filtered edge.

elements are observed in the normal output shown in Fig. 5.7(a). This hologram consists of 24 elemental holograms, 4 in horizontal and 6 in vertical. Since the object is assumed as the collection of self-illuminated points, such gaps might be caused sampling errors of points between elements. Figure 5.7(b) shows reconstructed image from the overlapped hologram without the digital filter with 10 % overlap in both vertical and horizontal. This hologram consists of 40 elemental holograms, 5 in horizontal and 8 in vertical. Obviously, bright strips appear in the reconstructed image because the overlapped areas are recorded twice and it makes the overlapped areas brighter. Figure 5.7(c) shows reconstructed image from the overlapped hologram with the digital filter (10 % overlap in both vertical and horizontal). One can find that the boundaries between elements are less visible than other results. Compare with these three different simulation results, the overlapped one with digital filter shows higher image quality than others.

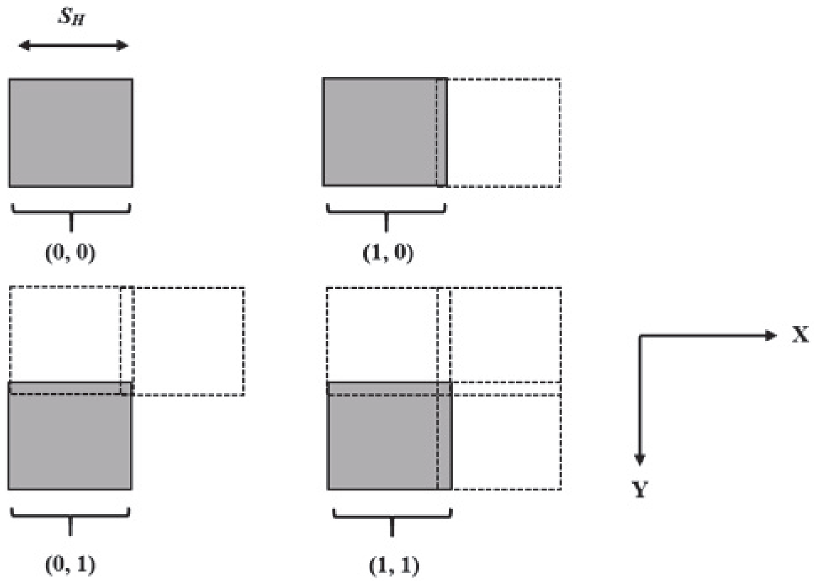

Figure 5.6: Partially overlapping approach 10% both in horizontal and vertical.

Figure 5.8 shows numerical reconstruction simulations of 3D model (skull) from normal, overlapped holograms without filter and with filter. All of these holograms consist of 60 elemental holograms, 6 in horizontal and 10 in vertical. Therefore, the printing time of all holograms will be the same. Figure 5.8(a) shows the result of normal output without overlapping. The simulation has been done with perfect alignment of elemental holograms, however, the split lines among each elemental holograms are still obviously. With 10 % in horizontal and 10 % in vertical of overlapping, the images without filter and with filter are shown in Fig. 5.8(b), 5.8(c), respectively. Bright grid appears in Fig. 5.8(b), which is caused by the intensity non-uniformity, of which the digital filter is not applied. In contrast, intensity fluctuations become smaller with the digital filter as shown in Fig. 5.8(c). Compare with these three different simulation results of 3D skull model, the overlapped one with digital filter shows higher image quality than others.

On the basic of faster printing speed and higher image quality, different simulations have been done. According to these results, Figs. 5.7(c) and 5.8(c) show higher image quality. It turns out that the proposed filter is effective to improve image quality of the volume hologram printer.

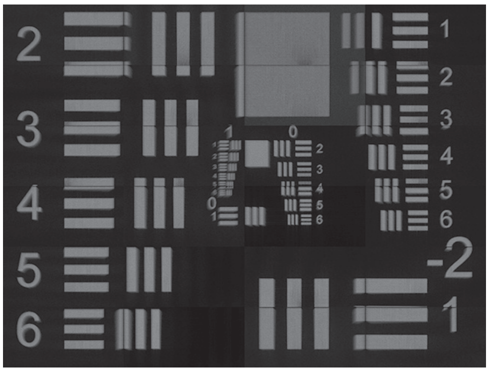

(a) Normal output without overlapping.

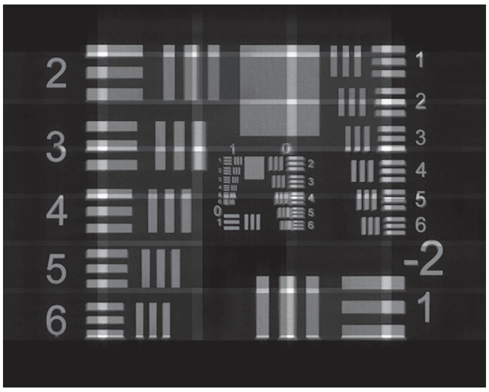

(b) 10 %, 10 % overlapping without filter.

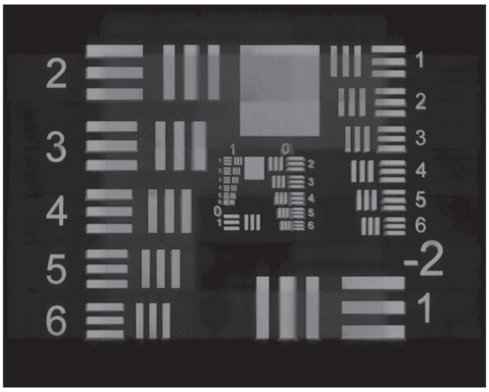

(c) 10 %, 10 % overlapping with filter.

Figure 5.7: Reconstructed images from USAF-1951 resolution chart.

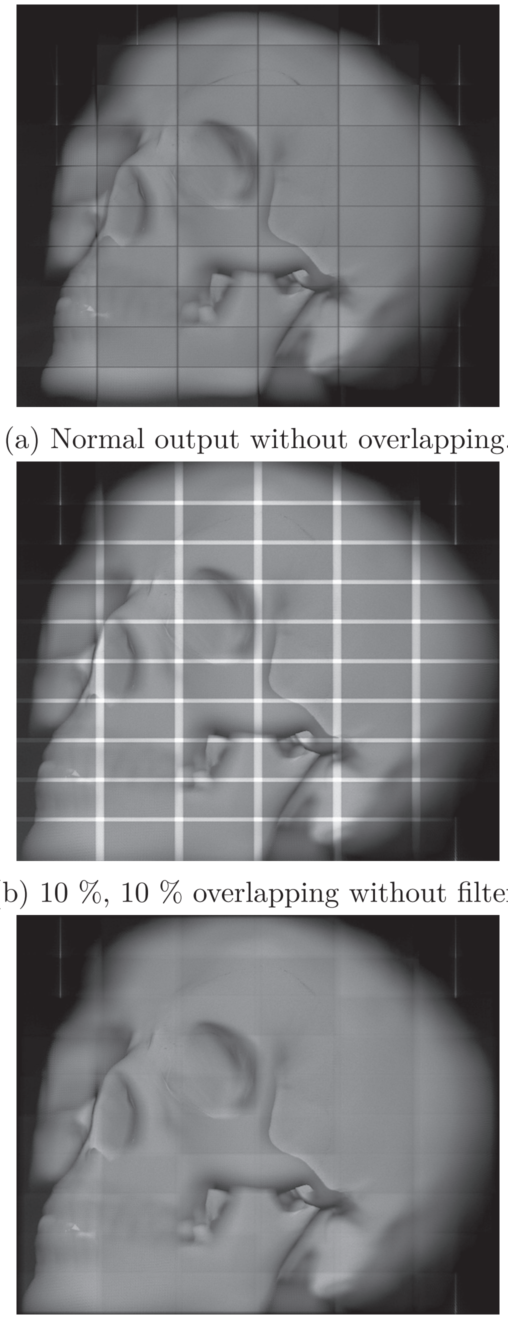

(a) Normal output without overlapping.

(b) 10 %, 10 % overlapping without filter.

(c) 10 %, 10 % overlapping with filter.

Figure 5.8: Reconstructed images from 3D skull holograms.

Chapter 6

Conclusion

This dissertation is focused on the improvement of image quality. In more detail, partially overlapping approach with a spatial digital filter was documented. In addition, the improved generation method of the improved optical system and intensity non-uniformity counterbalance are proposed.

In the first half of this paper, the principle and application of different holographic technology are mainly introduced. Due to the limitations of holography, the volume hologram is more widely applied due to its wavelength selectivity. On the basis of the original system, the improved system with a $4f$ system is modified and rebuilding. Meanwhile, full-color volume hologram printer system are proposed by our lab.

Since the hologram printer records many mm order's elemental holograms tiled in both horizontal and vertical directions, intensity fluctuations between elemental holograms will cause problems. To reduce these influences of phase discontinuity and image degradation caused by the movement of X-Y motorized stage, overlapping approach is applied.

However, if the mm order's transferred holograms are simply overlapped partially, there will have strong intensity non-uniformity (higher intensity in the overlapped parts than the non-overlapped parts) that causes the split lines and reduces the quality. To counterbalance the intensity near its edge, a spatial digital filter is proposed. Then a spatial digital filter is multiplied with the first hologram which is calculated as the lensless Fourier hologram. When printing, each elemental hologram need to be printed four times of the overlapped parts. Since the overlapping approach will cause the printing speed be slower, partially overlapping approach with 10% in both vertical and horizontal directions is proposed.

In summary, the improved methods of the image quality using partial overlapping was proposed and described in this paper.Then in order to improve the image quality of volume hologram printer, partial overlapping with 10% in both vertical and horizontal directions approach multiplied with a digital spatial filter is proposed in this paper. As a result of simulation, it shows that it could control the intensity around the edges of the reconstructed image from the hologram. The reconstructed image from the first hologram is recorded as the volume hologram, and volume holograms are tiled with partial overlapping. The limitation of the proposed method is that the overlap ratio has a trade off between compensation and printing speed. Compared with the numerical experimental results of partial overlapping with a digital filter and normal outputs, the proposed method shows effectiveness which makes it feasible to be applied in our future work.

Bibliography

[1] R. J. Collier, C. B. Burckhardt and L. H. Lin: "Optical Holography," Academic Press (1971).

[2] D. Gabor, "A New Microscopic Principle," Nature 161(4098), 777-778 (1948).

[3] D. Gabor, "Microscopy by reconstructed wavefronts," Proc. R. Soc. London Ser. A, 197(1051),454-487 (1949).

[4] Y. N. Denisyuk, "Photographic reconstruction of the optical properties of an object in its own scattered radiation field," Sov. Phys. Dokl., 7, 543 (1962).

[5] E. N. Leith and J. Upatnieks, "Wavefront reconstruction with diffused illumination and three – dimensional objects," J. Opt. Soc. Am., 54, 1295-1301 (1964).

[6] E. N. Leith and J. Upatnieks, "Wavefront reconstruction with continuous tone objects," J. Opt. Soc. Am., 53, 1377-1381 (1963).

[7] E. N. Leith and J. Upatnieks, "Reconstructed wavefronts and communication theory," J. Opt. Soc. Am., 52, 1123-1130 (1962).

[8] E. N. Leith, "the legacy of dennis gabor," Opt. Eng., 19(5), 195633 (1980).

[9] B. J. Chang, W. S. Colburn, C. D. Leonard, J. Lewis and J. A. Loses, "Holographic optical combiners for head-up displays," AD-A047998.

[10] B. J. Chang and C. D. Leonard, "Dichromated gelatin for the fabrication of holographic optical elements," Appl Opt., 18(14), 2407-2417 (1979)

[11] J. J. Couture and R. A. Lessard, "Intermittent characteristic curves for Kodak 649F plates at 514.5 nm," Appl Opt., 18(21), 3644 (1979).

[12] T. A. Shankoff and R. K. Curran, "efficient, high resolution, phase Diffraction gratings," Appl. Phys. Lett., 13, 239 (1968)

[13] B. J. Chang, "Dichromated Gelatin Holograms And Their Applications," Opt. Eng., 19(5), 195642 (1980).

[14] K. Snow and R. Vandewarker, "On using holograms for test glasses," Appl. Opt., 9, 822-827 (1970).

[15] B. A. Tozer, R. Glenville, A. L. Gordon, M. J. Little, J. M. Webster and D. G. Wright, “Holography applied to inspection and measurement in an industrial environment,” Opt. Eng., 24(5), 245746 (1985).

[16] M. J. R. Schwar, T. P. Pandya and F. J. Weinberg, “Point holograms as optical elements,” Nature, 215(5098), 239-241 (1967)

[17] D. H. Close, “Holographic optical elements,” Opt. Eng., 14(5), 145402 (1975).

[18] W. Lukosz, “Equivalent-lens theory of holographic imaging,” J. O. S. A., 58(8), 1084-1091 (1968).

[19] M. J. R. Schwar, T. P. Pandya and F. J. Weinberg, “Point holograms as optical element,” Nature, 215(098), 239-241 (1967)

[20] J. W. Goodman, R. W. Lawrence, “Digital image formation from electronically detected holograms,” Appl. Phys. Lett., 1(3), 77-79 (1967).

[21] M. H. Horman, “An Application of Wavefront Reconstruction to Interferometry,” Appl. Opt., 4(3), 333-336 (1965).

[22] R. L. Powell and K. A. Stetson, “Interferometric vibration analysis by wavefront reconstruction,” J. Opt. Soc. Am., 55(12), 1593-1597 (1965).

[23] K. A. Stetson and R. L. Powell, “Interferometric Hologram Evaluation and Real-Time Vibration Analysis of Diffuse Objects,” J. Opt. Soc. Am., 55(12), 1694-1695 (1965).

[24] J. M. Burch, “The application of laser in production engineering,” Prod. Eng., 44, 431-435 (1965).

[25] R. J. Collier, E. T. Doherty and K. S. Pennington, “Application of moire techniques to holography,” Appl. Phys. Lett. 7(8), 223-225 (1965).

[26] K. A. Haines and B. P. Hildebrand, “Surface-Deformation Measurement Using the Wavefront Reconstruction Technique,” Appl. Opt., 5(4), 595-602 (1966).

[27] R. E. Brooks, L. O. Heflinger and R. F. Wuerker, “Interferometry with a holographically reconstructed comparision beam,” Appl. Phys. Lett. 7(9), 248-249 (1965)

[28] J. E. Pearson, “Atmospheric turbulence compensation using coherent optical adaptive techniques,” Appl. Opt., 15(3), 622-631 (1976)

[29] S. Ma, D. Guthals, P. Hu and B. Campbell, “Atmospheric-turbulence compensation with self-referenced binary holographic interferometry,” J. Opt. Soc. Am., 11(1), 428-433 (1994).

[30] H. Fein, “Applications of holographic interferometryto structural and dynamic analysis of an advanced graphite-epoxy composite component,” Opt. Express, 3 (1), 35-44 (1998).

[31] G. M. Lai, H. Tsukasa, I. Kazuo, T. Takayoshi and T. Akira, “Three-dimensional reconstruction of electric-potential distribution in electron-holographic interferometry,” Appl. Opt., 33(5), 829-833 (1994)

[32] A. Nieves, A. Pilar and Q. Manuel, “Velocity measurements in a convective flow by holographic interferometry,” Appl. Opt., 36(27), 6997-7007 (1997)

[33] A. P. Tzannis, P. B. H. M. Frey, T. Gerber, B. Mischler and P. P. Radi, “Phase-conjugate resonant holographic interferometry applied to NH concentration measurements in a two-dimensional diffusion flame,” Appl. Opt., 36(30), 7978-7983 (1997)

[34] X. D. Xiao and I. K. Puri, “Systematic Approach Based on Holographic Interferometry Measurements to Characterize the Flame Structure of Partially Premixed Flames.” Appl. Opt., 40(6), 731-740 (2001)

[35] T. Diana, “Homogeneity testing of optical glass by holographic interferometry,” Appl. Opt. 30(7), 752-755 (1991).

[36] S. Leopoldo, C. Hernán and S. Maurice, “Eight-frame holographic interferometry system for transient plasma diagnostics,” Appl. Opt., 34(34), 7831-7833 (1995)

[37] R. B. Owen and A. A. Zozulya, “Comparative Study with Double-Exposure Digital Holographic Interferometry and a Shack-Hartmann Sensor to Characterize Transparent Materials,” Appl. Opt., 41(28), 5891-5895 (2002)

[38] A. Rebane and J. Aaviksoo, “Holographic interferometry of ultrafast transients by photochemical hole burning,” Opt. Lett., 13(11), 993-995 (1988)

[39] A. Choudry, “Digital holographic interferometry of convective heat transport,” Appl. Opt., 20(7), 1240-1244 (1981)

[40] S. Grilli, P. Ferraro, S. De Nicola, A. Finizio, G. Pierattini and R. Meucci, “Whole optical wavefields reconstruction by digital holography,” Opt. Express, 9, 294-302 (2001)

[41] Takeshi Yamaguchi and Hiroshi Yoshikawa, “Computer-generated image hologram” , Chinese Optics Letters, COL 9(12), 120006(2011)

[42] Engineering optics. No.4 (in Chinese)

[43] J. P. Waters, “Holographic image synthesis utilizing theoretical methods,” Appl. Phys. Lett. 9(11), 405 – 407(1966).

[44] G. L. Rogers, “Gabor diffraction microscopy: the hologram as a generalized zone-plate,” Nature 166(4214), 237(1950).

[45] H. Yoshikawa and T. Yamaguchi, “Computer-generated holograms for 3D display,” Chin. Opt. Lett. 7,1079 (2009).

[46] H. Yoshikawa,and T. Yamaguchi, "Review of Holographic Printers for Computer-Generated Holograms," IEEE Transactions on Industrial Informatics, 12(4), 1584–1589. https://doi.org/10.1109/TII.2015.2475722 (2016).

[47] Jianpin Xie, "Laser holography and cultural relics protection," Applied laser, 1983, 01:41-42.

[48] Bingheng Xiong, Dingjun Guo, "Recent development of giant holography," Progress in laser and Optoelectronics, 1991, 07:25-26.

[49] Jianpin Xie, et al. "General situation and development trend of foreign printing holography," Progress in laser and Optoelectronics, 1991, 09:3-7.

[50] Bartolini R, et al. "Embossed hologram motion pictures for television playback." Applied Optics, 1970, 9(10):2283-2290.

[51] Haines K A. "Development of embossed holograms." Proc,SPIE.1996,2653:45-52.

[52] Svetlana S S, Dejan P. "Relief hologram replication using a dental composite as an embossing tool." Optics Express, 2005, 13(7):2747-2754.

[53] H. Kang, Y. Kim, J. Park, E. Stoykova, and S. Hong, "Color holographic wave-front printing method based on partitioned elemental hologram," in Proc. Imag. Appl. Opt., [CD-ROM], Paper no. DTh3B.1 (2014).

[54] T. Yamaguchi, O. Miyamoto and H. Yoshikawa: "Volume hologram printer to record the wavefront of three-dimensional objects," Optical Engineering, vol. 51, no. 7, pp. 075802(1-7) (2012).

[55] K. Wakunami, R. Oi, T. Senoh, H. Sasaki, Y. Ichihashi, and K. Yamamoto, "Wavefront printing technique with overlapping approach toward high definition holographic image reconstruction," In B. Javidi & J.-Y. Son (Eds.), Proc. SPIE 9867, Three-Dimensional Imaging, Visualization, and Display 2016 (p. 98670J). https://doi.org/10.1117/12.2229517 (2016).

Dedication

This thesis is dedicated to my girlfriend, Shi Lili. Although we live in different places, she still accompany me on the rocky road for the future, and supported me in innumerable ways. As time is closing, we are going to get married. Since the road of our love is filled with frustrations, we get to know each other more profound and it makes our relationship much stronger. Years hence, we will remember this time while thanking to our life.

Genial thanks to Dad, Mom and my relatives.

Acknowledgments

Ph.D. study is a journey full of memories. It not only allows me to acquire deeper knowledge, but also strengthens author's path in future life. As this life is going to end, there have both the pleasure of relief and the anxiety of loss. Fortunately, with the guidance of the instructor, the care of relatives and the encouragement of friends, this research is going to be completed. The author gratefully acknowledges to Professor Hiroshi Yoshikawa for his guidance, encouragement and supporting this work, and other devoted examiners for reviewing this thesis and giving very helpful advice.

Thanks also to other professors and teachers in the Department of Computer Engineering, College of Science and Technology, Nihon University.

Thanks also to Professor Hiroyuki Hosono and Associate Professor Takeshi Yamaguchi for their lots of discussions and help, and to members of Yoshikawa & Yamaguchi Laboratory.

Publications

Reviewed Journal Paper

1. Hua, H., Yamaguchi, T., and Yoshikawa, H.: "Partially Overlapping Printing with Digital Filter to Improve Quality of Volume Hologram Printer − Numerical Simulation −," Applied Sciences, 10(11), 3963. https://doi.org/10.3390/app10113963 (2020).

International Conference

1. Hua, H., Yamaguchi, T., and Yoshikawa, H.: "Partially Overlapping Printing to Improve Image Quality of Volume Hologram Printer − Numerical Simulation −," Digital Holography and Three-Dimensional Imaging 2019, W3A.29. https://doi.org/10.1364/dh.2019.w3a.29 (2019).

Co-authored paper

1. Di, H.; Wang, Q.; Hua, H.; Li, S.; Yan, Q.; Liu, J.; Song, Y.; Hua, D. Aerosol Microphysical Particle Parameter Inversion and Error Analysis Based on Remote Sensing Data. Remote Sens. 2018, 10, 1753.

2. Huige Di, Zhanfei Zhang, Hangbo Hua, Jiaqi Zhang, Dengxin Hua, Yufeng Wang, and Tingyao He, "Optimization design of spectral discriminator for high-spectral-resolution lidar based on error analysis," Opt. Express 25, 5068-5080 (2017)

3. Huige Di, Hangbo Hua, Yan Cui, Dengxin Hua, Tingyao He, Yufeng Wang, Qing Yan. Vertical distribution of optical and micro-physical properties of smog aerosols measured by multi-wavelength polarization lidar in Xi' an, China. Journal of Quantitative Spectroscopy & Radiative Transfer. 188, 28-38(2017)

4. HUIGE DI, HANGBO HUA, YAN CUI, DENGXIN HUA, BO LI, AND YUEHUI SONG. Correction technology of a polarization lidar with a complex optical system. Journal of the Optical Society of America A. Vol.33, No.8, pp. 1488-1494 (2016)